PROCEEDINGS - 5WCEE

1973

EMPIRICAL AND THEORETICAL STUDY OF NEAR-FAULT WAVE PROPAGATION[1]

by

David M. Boore[2]

SYNOPSIS

The well defined trends of peak ground motion at distances beyond 10-20 km and the sparsity of data for closer distances and for very large earthquakes invite investigation of the dependence of strong ground motion on physical processes of faulting and wave propagation. Toward this end, a number of empirical and theoretical studies are being pursued. Results of present studies isolate some of the critical parameters, and point up the difficulty of making general predictions of the ground motions near faults defined only by a few parameters, such as magnitude and fault length.

INTRODUCTION

The 1969 Santa Rosa (m = 5.6 and 5.7, $6 million damage) and the 1971 San Fernando (m = 6.6, $500 million damage) earthquakes in California and the 1972 Managua, Nicaragua (m = 5.6) earthquake are recent sobering reminders of the large potential for damage from even moderate-sized shocks in urban areas. Because of the hazard to life and property in urban areas, the increasing demand for nuclear power plants in regions that are tectonically active, and the trend toward optimizing the seismic design of public structures, an accurate determination of seismic loading imposed by nearby earthquakes is essential. A major concern of engineering seismologists then, is the behavior of the various parameters of strong ground motion, such as peak acceleration, velocity, displacement, and some measure of duration, at distances within 10-15 km of an earthquake-producing fault. Commonly used empirical curves based on pre-1971 data generally underestimate the sparsity of data for the close-in region (Boore and Page, 1972). On the other hand, extrapolation of the well-defined acceleration-distance trends established from data at moderate distances leads to unrealistically high accelerations near the causative fault. A number of theoretical and empirical studies have been undertaken to increase our understanding of the attenuation of ground motion in the region close to the fault. The results reported here represent work in progress.

DATA

A plot of peak horizontal acceleration for earthquakes for which the distance to faulting is established to within 5 km (Fig. 1) shows remarkably consistent trends: at any given distance beyond 10-20 km, the values in general increase with magnitude, and the data for all magnitudes show a uniform attenuation at a rate of $r^{-1.4}$ to $r^{-1.8}$. For dis-

---

[1] Publication authorized by the Director, U. S. Geological Survey

[2] Assistant Professor of Geophysics, Stanford University, Stanford, Ca. and Geophysicist, U. S. Geological Survey, Menlo Park, Ca.

tances within 10-15 km the few available data points suggest a flattening of the attenuation curve as the fault surface is approached. The distance used in the plot is the closest distance between the strong motion site and the fault surface, usually the zone of surface breakage. If, as seems plausible, much of the strong shaking is caused by a zone of energy release at depth, then the apparent flattening could be an artifact of the distance measure. There are other possible explanations of a zone of flattening, some of these are discussed below. For the data plotted in Fig. 1, only well-located earthquakes have been used. A number of other recordings have been obtained, but the uncertainty in location of the earthquakes is often no better than 25 km. The scatter due to such uncertainty can easily obscure the well defined trends seen in the plot (Page and others, 1972). The data show, with a few possible exceptions, no obvious correlations with site geology; the scatter in bedrock values is as great as between alluvium and bedrock sites. A preliminary analysis of peak horizontal velocity, however, suggests a much stronger dependence of the data on site geology. This could contribute to the scatter in the data used for the velocity-distance plot (Fig. 2). Despite the scatter, the data appear to separate with magnitude; the attenuation with distance seems to be less rapid than for acceleration.

The attenuation properties due to transmission path are being studied by analysis of S vaves from many small, well-located earthquakes near San Benito, California, recorded on three-component portable seismograph units. As the events may be considered point sources, finiteness is eliminated. The recordings are made for distances of strong motion interest: less than 5 km to more than 50 km. The ground motions from large and small earthquakes in this distance range should have in common some propagation paths, and study of the small events may give us some insight into the attenuation relations for large events. Peak motion for two events (m = 2) recorded east and west of the epicenters shows consistent decay at a relatively high rate (Fig. 3). The decay rate is much faster than that given by strong motion recordings. Part of this probably reflects the influence of inelastic absorption; the small ground motions are characterized by frequencies near 10 Hz, which would have greater attenuation than the 3-5 Hz energy characteristic of most strong motion accelerograms. ~~It does not seem possible to account for the difference solely on this basis.~~ The discrepancy may also reflect a greater partitioning of energy into guided waves for the large earthquakes. These waves would decay less rapidly than the body waves.

A study of transmission properties of energy in different frequency bands is also being made for various strong motion recordings of moderate earthquakes. Use of band-pass filters on accelerograms recorded during the Parkfield earthquake of 1966 reveals some interesting features and emphasizes the complexity of the near-field motions from rupturing faults of finite size (Figs. 4,5, & 6). The waveforms are arranged according to distance from epicenter. The relative positions in time are determined by a tentative identification of the S wave from the epicenter, as most of the instruments apparently did not trigger on the initial P motion. Of more interest to us here is the decay of motions in the various frequency bands (Fig. 7). The unfiltered peak values suggest a region of little attenuation. This apparent plateau is defined primarily by the one recording close to the fault (site w). When looked at in detail,

it is seen that the frequency structure of this motion is quite different from that at other sites; the motion in the frequency band contributing most to the peak acceleration at site 2 decays more rapidly than indicated by the unfiltered peak acceleration. Moreover, the peak accelerations at the other sites are controlled to a great extent by the higher frequency motions. These high-frequency motions apparently increase with distance from the fault! It may be that a complex interaction of various wave types due to the propagating rupture, coupled with anomalous inelastic absorption near the fault zone and possibly site effects have fortuitously produced a simple pattern of attenuation of the peak unfiltered accelerations. The apparent plateau is not obviously related to fault geometry. From the acceleration-distance plot (Fig. 1), however, it is evident that beyond 10 km the peak accelerations for recordings out to more than 100 km from the fault show a consistent attenuation with distance; the filtered motions at sites 8 and 12 agree with this.

THEORY

Although the complexities of the motions near the fault make it difficult to predict the details of the ground motion, various simplified studies are useful in understanding the dependence of the motion on the physical parameters. For example, it is clear that extrapolation of the apparent power-law attenuation to the fault surface leads to unrealistically large ground motions. Several studies relate the peak ground motions at the fault surface to various mechanisms of faulting (Ambraseys, 1969; Housner, 1965; Brune, 1970; Ida, 1973). A finite limit at the fault surface corresponds to a flattening in the attenuation curves close to the fault. The maximum velocity and accelerations suggested by the various studies are shown in normalized form in Fig. 8. The peak velocity depends on material density and rigidity and the effective stress released at the fault surface. The peak acceleration, on the other hand, depends on high-frequency cutoff also, as very large accelerations are possible if the high-frequency motion is not attenuated. It appears that motions produced by most earthquakes do not contain these high frequencies, although the data supporting this is sparse. An absence of high frequencies and a consequent limit on acceleration may be due to both the mechanics of rupture (Ida, 1973) and anomalous inelastic absorption of energy in the highly sheared zones surrounding major faults.

Inelastic absorption of energy will control the attenuation of the motions with distance. A simulation of propagation of the pulses of velocity and acceleration corresponding to the source model of Brune (1970) in a lossy material shows that the effect of absorption is much less critical for peak velocity than peak acceleration (Fig. 9). Since a strict application of Brune's model gives infinite peak accelerations, all the energy above a given cutoff frequency was removed. All the attenuation with distance shown (Fig. 9) is due to absorption; there is no geometric attenuation in this model. Note that the peak values are controlled by a fairly broad range of frequencies, indicating that the apparent attenuation is not simply given by a decaying exponential at a given grequency. It was for this reason that a model of the source was used that produced a waveform in the time domain consistent with current concepts of source spectra.

Aside from inelastic absorption and transmission path effects due to

layering of the crust, another critical control in the behavior of the near-field motions is the geometry and kinematics of faulting. If faulting takes place instantaneously over the entire rupture surface (Brune, 1970), or occurs randomly in space and time over the surface (Housner, 1955), little attenuation of the motions due to the kinematics of faulting should occur before a distance comparable to the fault dimensions is reached. At greater distance for uniform, perfectly elastic material of infinite extent, the fault will appear as a point source with attenuation proportional to r^{-1}. This and the role of effective stress discussed earlier, suggest a simple scaling of the ground motions dependent on characteristic source size, effective stress, and high-frequency cutoff (Dieterich, these proceedings). This scaling is more physical than that obtained by using magnitude, for it is possible for two events to have the same magnitude but different effective stresses and thus different peak ground motions. Unfortunately, predictions of these source parameters are subject to large uncertainties, and how useful such scaling relations would be is not clear. Another difficulty involves scaling with source size. It was argued above that for certain time histories of faulting the near-field ground motions do not depend strongly on distance to faulting. For more coherent rupture, this may no longer be true since at any distance the area of the fault contributing motions which define the peak motion may not increase at a rate proportional to distance from the fault. In this case, the motion should decay between r^0 (very close to the fault if accelerations at the fault surface are limited) and r^{-1}, but any break-over (corner) distances may not be directly related to fault dimensions. Similar considerations lead to the conclusion that the effect of the source dimensions becomes less important as the frequency of the motion of interest increases. Peak ground displacement should be much more sensitive to source dimensions than peak ground acceleration. Support for this conclusion comes from various dislocation models of faulting (Fig. 10). Peak displacements computed along a profile normal to the center of a unilaterally propagating fault are shown in Fig. 10. The 3-D results come from a fault of 10 units length and 2.5 units width (Haskell, 1969), the 2-D results from a fault of similar length but infinite width (Boore and Zoback, 1973). In both cases rupture occurred instantaneously over the entire width but propagated at a finite velocity over the length. The 3-D, 2-D comparison shows that the width of the fault is important for the peak displacements. It is of interest that the 2-D results give an apparent corner although the width is infinite. This corner seems to be related to the product of rise time and rupture velocity. A similar comparison of peak velocities is also given in Fig. 10 (no comparison of peak acceleration is given because of numerical inaccuracies). Here the two models show little width dependence at close-in points. Furthermore, it is apparent that displacement is decaying less rapidly with distance than peak velocity. These results emphasize that fault-dimension control of the attenuation of motion is a function not only of the details of rupture but also of the dominant frequencies of the motion.

CONCLUSION

Existing data for earthquakes to Richter magnitude 7-1/2 define peak accelerations to within about a factor of two at distances beyond 10-20 km from faulting. The behavior of the data at distances closer to the

fault is not as well established. Furthermore, recent work indicates that the commonly used abscissa given by closest distance to faulting may bear little relationship to the actual center of radiated energy, and that near-field radiation patterns can produce significant variations in the motions. Thus, we possibly should abandon the idea of a curve of ground motion against distance when close to faults and use instead a constant value for any particular parameter of motion. Attenuation relations, such as suggested in Figs. 1 and 2, can then be used for sites beyond this near-field "grey" zone.

Various theoretical arguments can aid our insight and help explain existing data but must be used with caution for prediction. It appears that in the near future some of the urgently needed near field data will be forthcoming. I expect that it will show considerable scatter, especially for the higher frequency parts of the motion where the seismic wavelengths are less than the fault dimensions and are comparable to dimensions of geologic heterogeneities. This close-in data, however, should prove very valuable in understanding the mechanics of faulting and hopefully can be used in more realistic simulations of ground motion than are now available.

Finally, any apparent bias in this paper to the use of peak acceleration as a parameter of ground motion is only a result of the availability and completeness of the data. Of course, ground motion cannot be adequately described by one parameter, just as an earthquake cannot be described by magnitude alone. We have been using the Newmark-Hall procedure to estimate response spectra and thus have parameterized the motion by peak displacement and velocity, as well as acceleration. Even this is incomplete, but seems to be a practical way of including frequency information with a small number of parameters.

ACKNOWLEDGEMENTS

Some of the research reported here was done on a NRC-USGS Post-Doctoral Research Associateship at the U.S. Geological Survey, Menlo Park, Calif. Several of the studies described are parts of investigations being carried out with David P. Hill of the U.S. Geological Survey and Alan Lindh of Stanford University.

REFERENCES

1. Boore, D. M., and R. A. Page, Accelerations near faulting in moderate-sized earthquakes, U.S. Geological Survey open file report, 13 pp., 1972.

2. Page, R. A., D. M. Boore, W. B. Joyner, and H. W. Coulter, Ground motion values for use in the seismic design of the Trans-Alaskan Pipeline System, U.S. Geological Survey Circular 672, 23 pp., 1972.

3. Ambraseys, N. N., Maximum intensity of ground movements caused by faulting, Proc. of Fourth World Conference on Earthquake Engineering, Santiago, Chile, v. 1, pp. 154-171, 1969.

4. Housner, G. W., Intensity of earthquake ground shaking near the causitive fault, Proc. of Third World Conference on Earthquake Engineering, v. 1, pp. III-94 - III-109, 1965.

5. Housner, G. W., Properties of strong ground motion earthquakes, Bull. Seism. Soc. Am., v. 45, pp. 197-218, 1955.

6. Brune, J. N., Tectonic stress and the spectra of seismic shear waves from earthquakes, J. Geophys. Res., v. 75, pp. 4997-5009, 1970.

7. Ida, Y., The maximum acceleration of seismic ground motion, Bull. Seism. Soc. Am. (in press), 1973.

8. Haskell, N. A., Elastic displacements in the near-field of a propagating fault, Bull. Seism. Soc. Am., v. 59, pp. 865-908, 1969.

9. Boore, D. M., and M. Zoback, Two-dimensional dynamic dislocation modeling of faults, Bull. Seism. Soc. Am. (in press), 1973.

ERRATA

p. 2, par. 1, line 15: A more complete analysis of the velocity data no longer suggests a strong dependence of velocity on site geology.

p. 3, par. 2: The first part of the last sentence should read "An absence of high frequencies and a consequent limit on acceleration may be due to the mechanics and kinematics of rupture...".

Fig. 10 caption: Read "total" for "peak" in line 1. Read "1.0 to 1.5" for "0.1 to 0.5" in line 10. Read "3D" for "2D" in line 10.

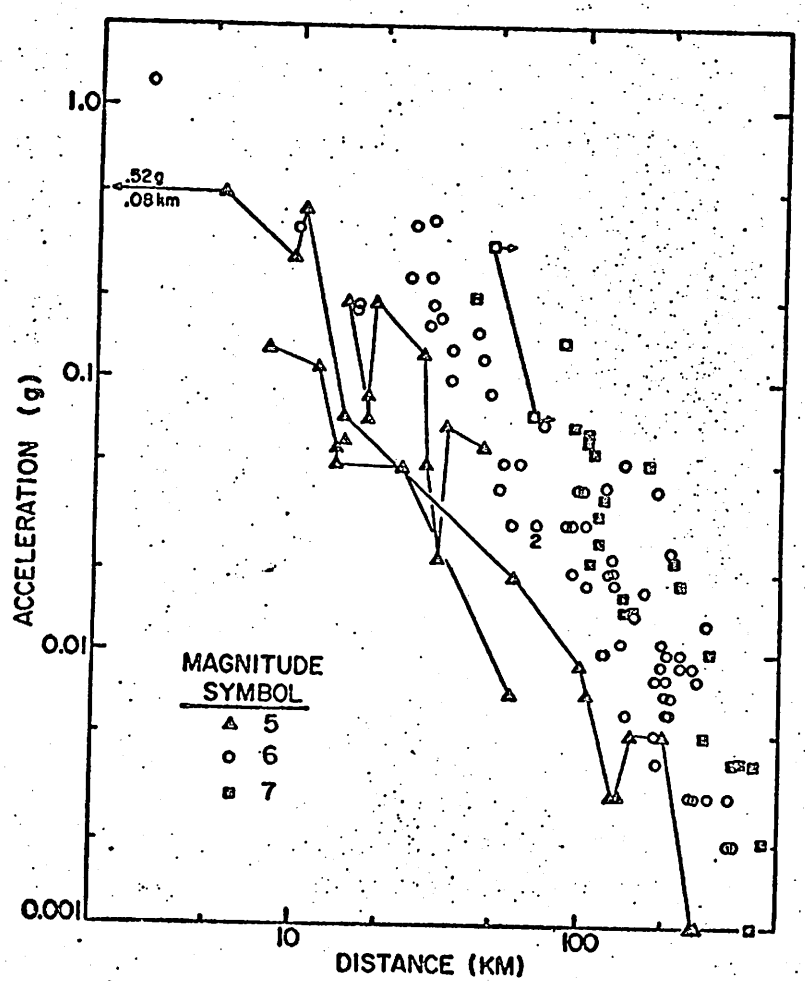

Fig. 1. Peak horizontal acceleration versus distance to slipped fault as a function of magnitude. Except for 1949 Puget Sound shock (open squares), data shown are those for which distances to fault are most accurately known. Straight-line segments connect observations at different stations for an individual earthquake, for three magnitude-5 shocks and one magnitude-7 shock. From top to bottom, suites of magnitude-5 data are from 1970 Lytle Creek (m = 5.4), Parkfield (m = 5.5), and 1957 Daly City (m = 5.3) shocks. Closest Parkfield data point lies off plot to left at 0.08 km. For magnitude 6, most data within 100 km are from 1971 San Fernando earthquake (m = 6.6), and most data beyond 100 km are from 1968 Borrego Mountain earthquake (m = 6.5). Most magnitude-7 data are from 1952 Kern County shock (m = 7.7). Open squares are values from 1949 Puget Sound event (m = 7.1), for which distances are determined to hypocenter assuming minimum focal depth of 45 km. Arrows denote minimum values (from Page and others, 1972).

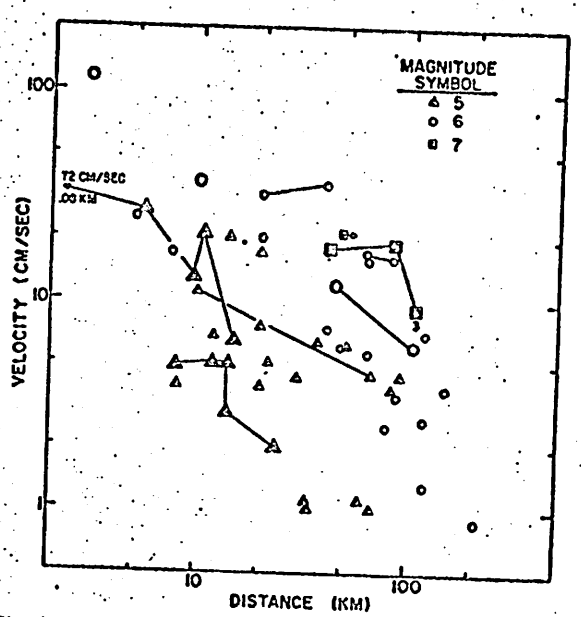

Fig. 2. Peak horizontal velocity versus distance to slipped fault, if known, or epicentral distance for magnitudes 5, 6 and 7. Uncertainties in distances are less than 5 km for larger symbols and more than 5 and possibly as large as 25 km for smaller symbols. Line segments connect data for individual shocks. The closest point to the fault for the Parkfield shock lies off the plot at 0.08 km. Arrows denote minimum values (from Page and others, 1972).

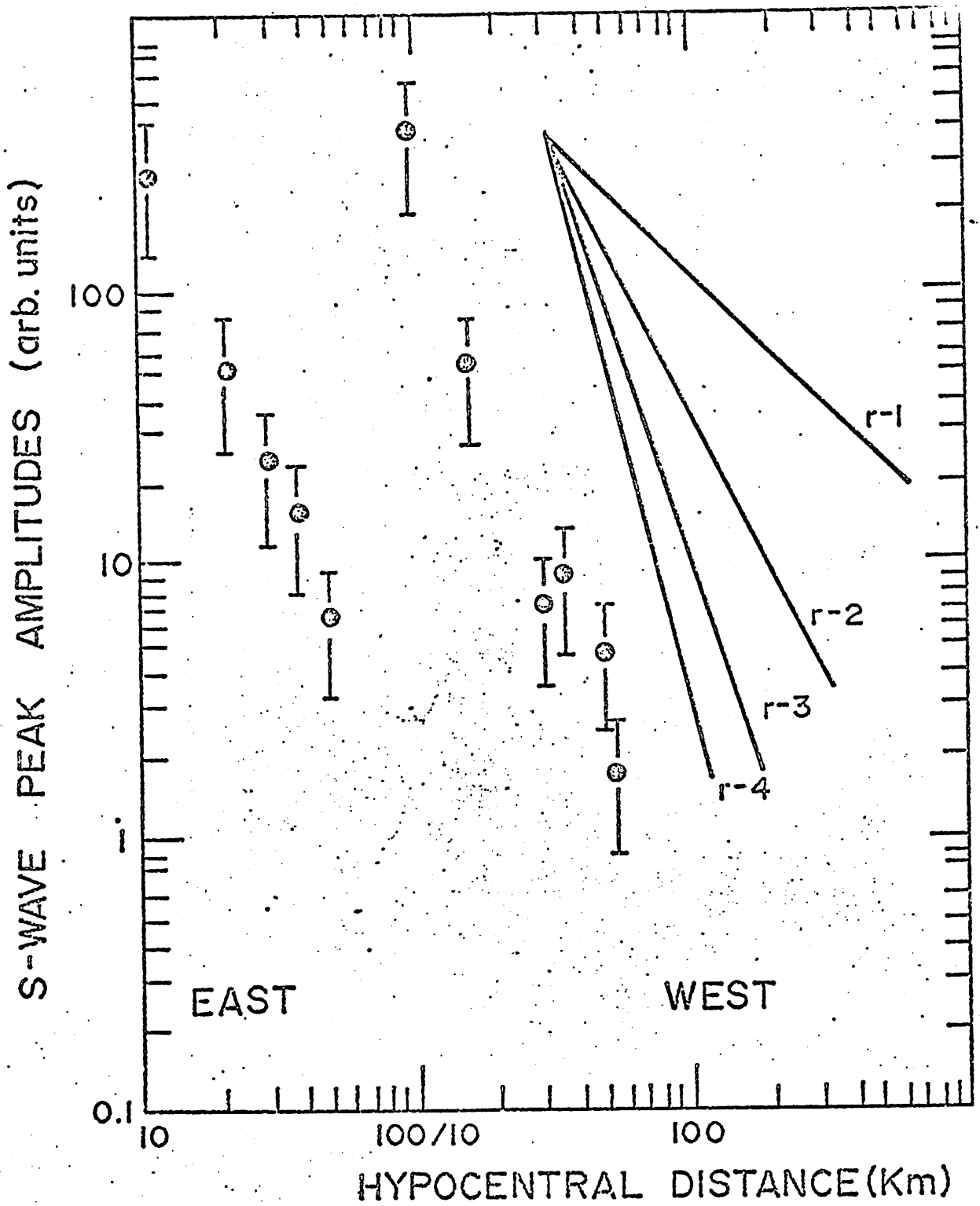

Fig. 3. Peak S-wave amplitudes recorded on a line to the east and a line to the west of the epicentral region for several small earthquakes near San Benito, Calif. Vertical bars denote estimated uncertainty of amplitudes on three-component recordings. Dominant frequency of motion is 11 Hz to the west and 8 Hz to the east.

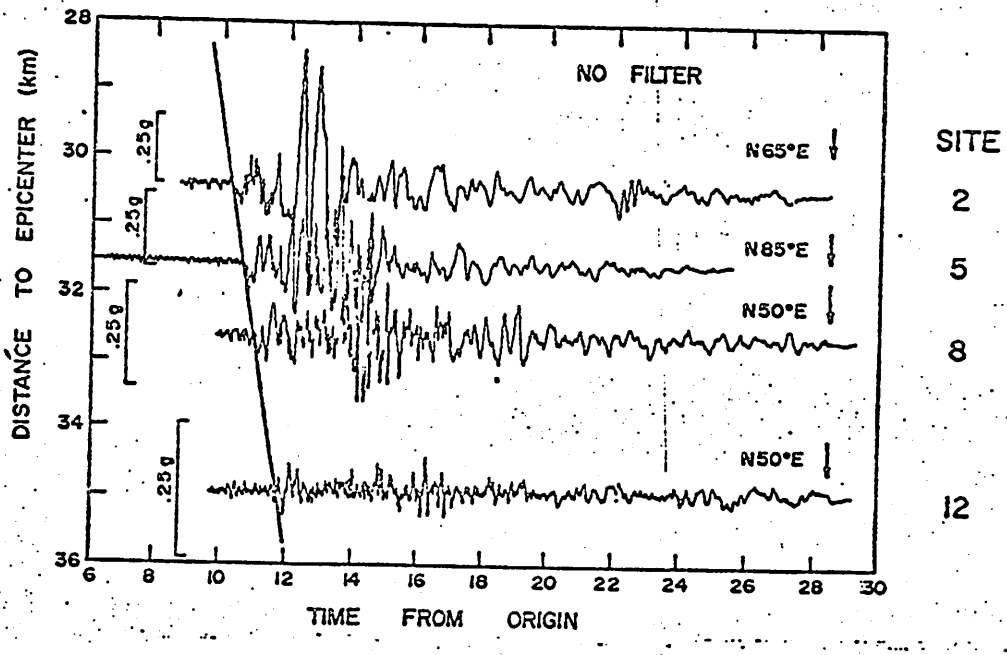

Fig.4. Unfiltered accelerograms for sites 2,5,8, and 12 from the Parkfield, California, earthquake of June 28, 1966, arranged according to epicentral distance. Time from the origin based on tentative identification of the S wave (solid slant line) and a velocity model for the region, assuming the initial P-motion triggered the instrument at site 5.

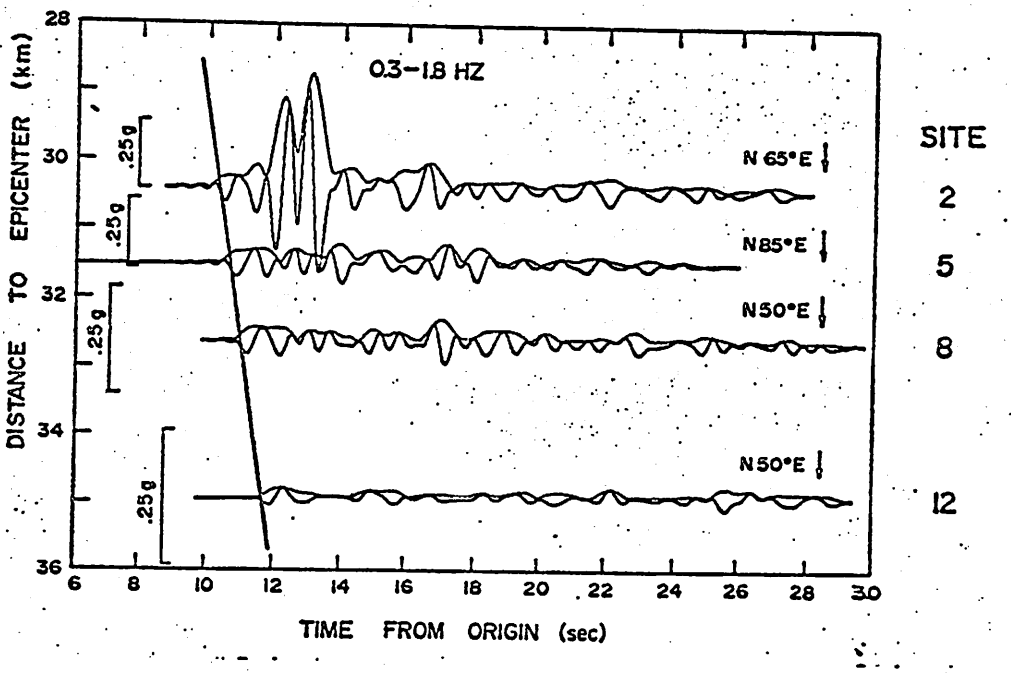

Fig.5. Accelerograms in Fig.4 after applying a band-pass filter with high- and low-frequency roll off points at 0.3 and 1.8 Hz. The envelope of the motion is also shown.

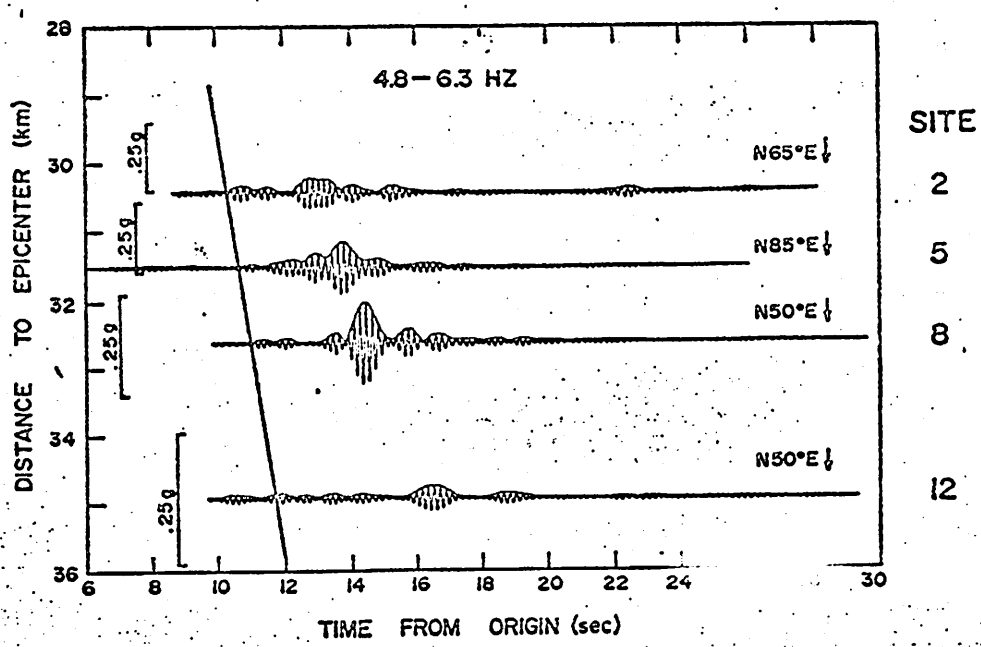

Fig.6. Accelerograms filtered with 4.8 and 6.3 Hz cutoff points.

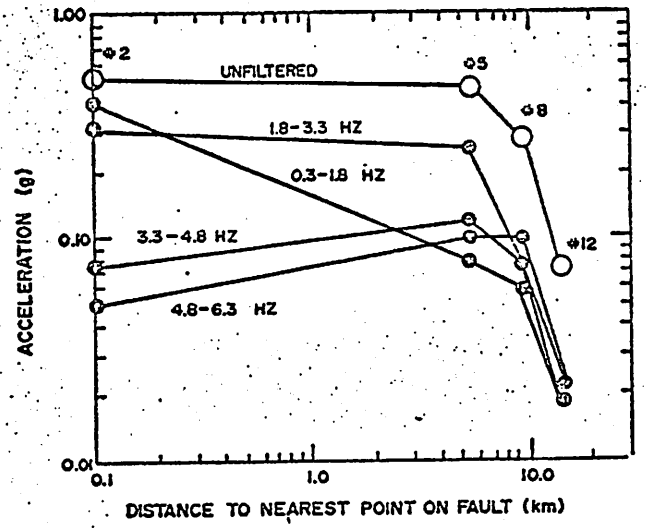

Fig.7. Maximum acceleration from the Parkfield earthquake at the 4 sites for a series of band-pass filters (indicated by the pair of numbers). The lines connecting the sites are for clarity of the various filter results and do not imply an interpolation of the data. The filter windows overlapped one another to an extent, and thus, for example, the 1.8-3.3 and 0.3-1.8 results are not inconsistent with the no filter acceleration at site 2.

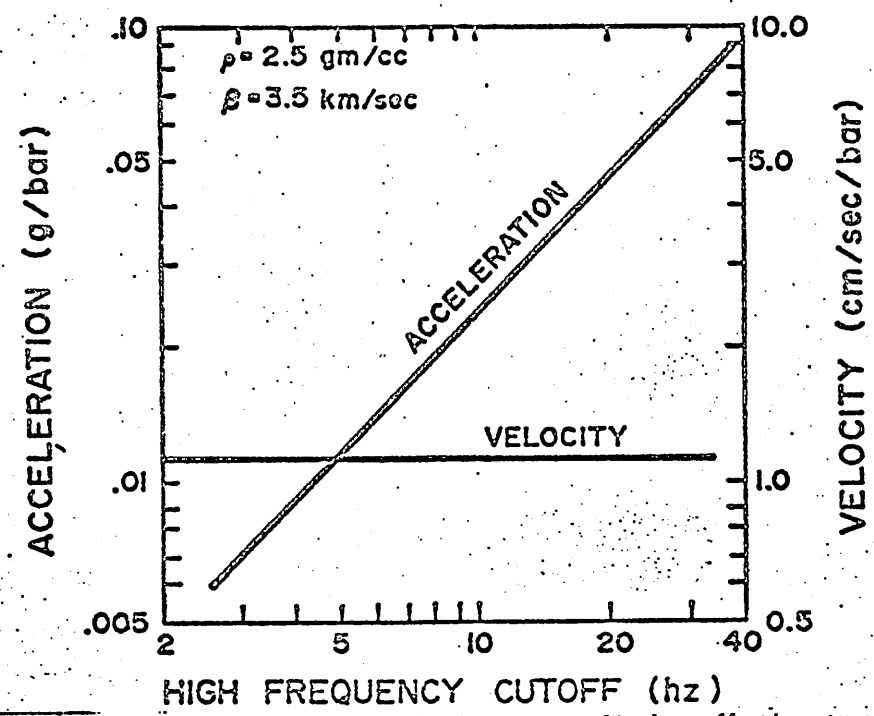

Fig. 8. Peak acceleration and velocity, normalized to effective stress, as a function of a high-frequency limit on the ground motions. The acceleration depends on the way in which the high frequencies are removed; in this case a rectangular window function is assumed. A box with corner of 10 Hz approximately predicts the same line as passing the ground motion through an accelerometer of 16 Hz free period and 0.6 damping. The values used for density (ρ) and shear velocity (β) are reasonable and are not expected to vary by much.

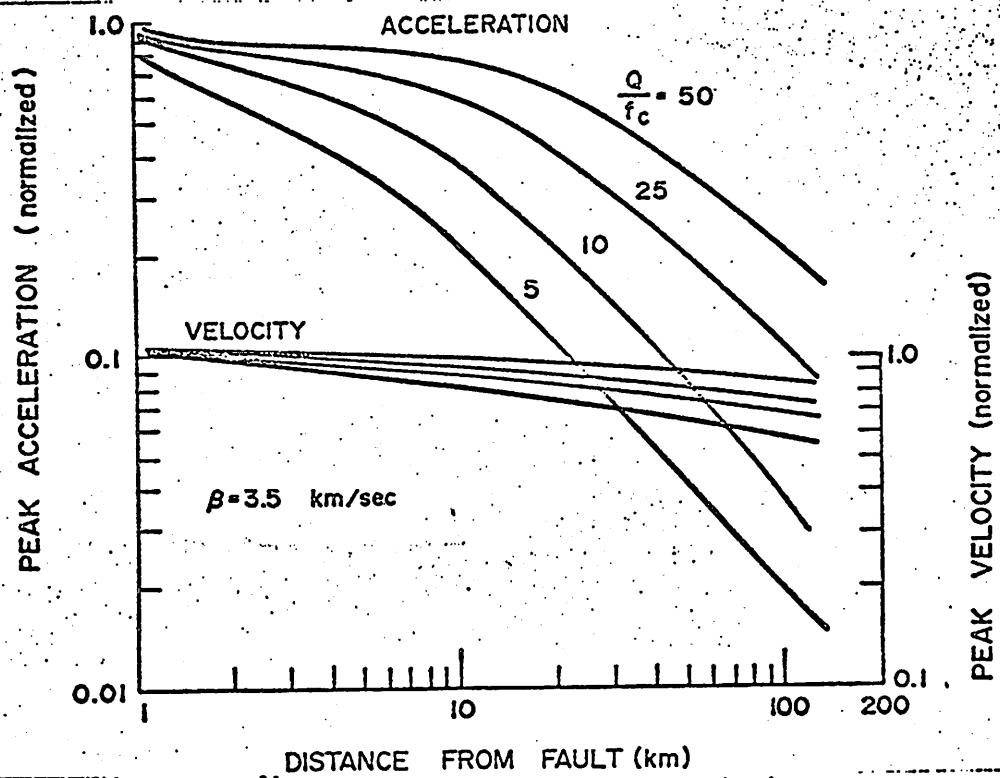

Fig. 9. Peak acceleration and velocity produced by the travel of a pulse through a lossy material. The inelastic absorption is characterized by the ratio of the quality factor Q and a measure of the high frequency cutoff, f_c. The pulse is consistent with Brune's near-field source model (Brune, 1970) for a rise time of 2 seconds. The high-frequency attenuation is achieved by passing the resulting ground motion through an accelerometer of free period proportional to f_c and a damping of 0.6.

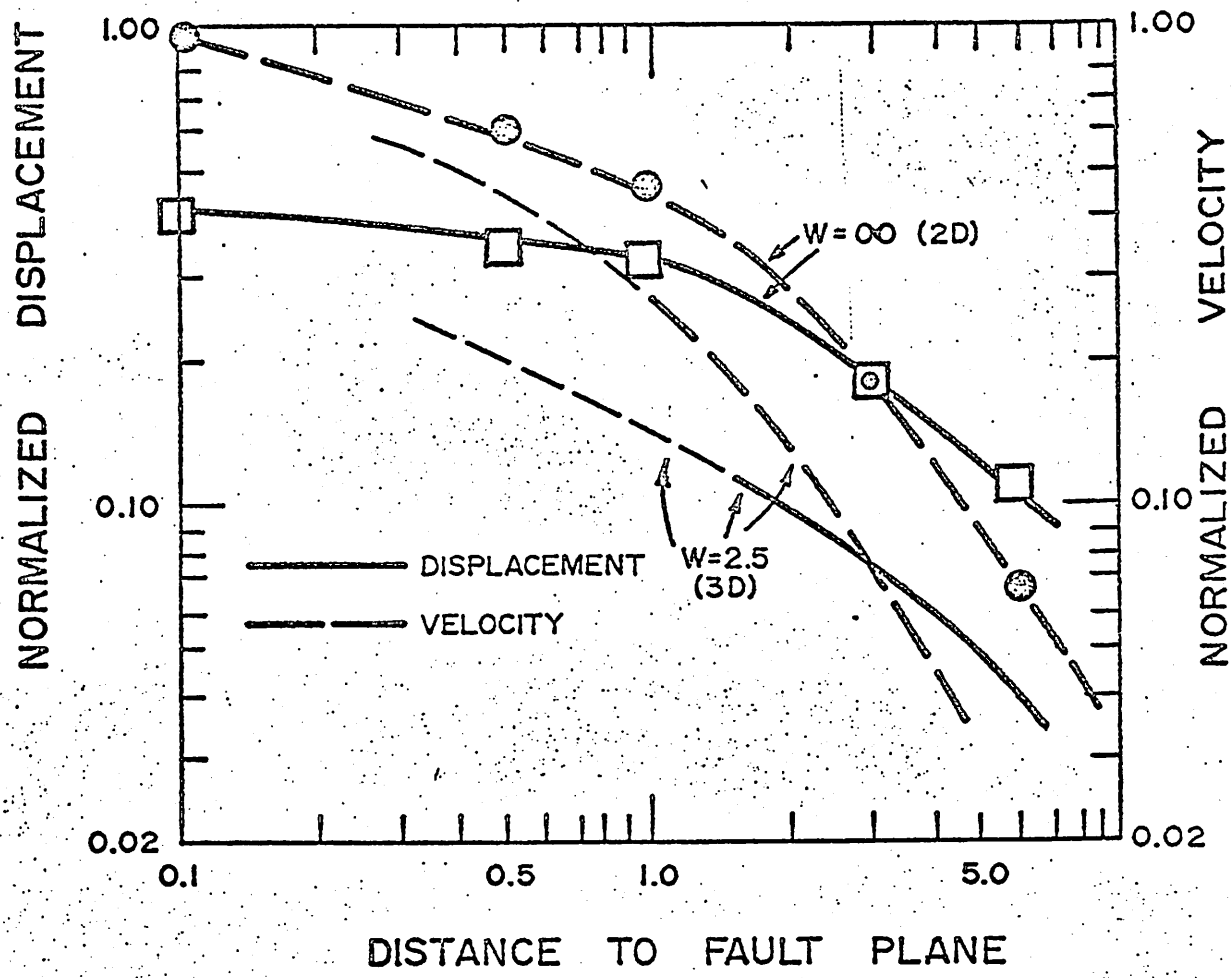

Fig. 10. Peak velocity (dashed line) and displacement (solid line) for the normal-component motions from dislocation models of uniform, unilateral rupture of a longitudinal shear fault of 10 units of length and 2.5 units width (3D model) and infinite width (2D model). In both cases the rupture velocity is 1 unit/sec and the dislocation function is a truncated ramp of 1 sec rise time. The amplitudes are taken normal to the fault starting from a point in the middle of the fault plane 6 units from the point of initial rupture. The motions are normalized to the maximum displacement and velocity of the dislocation function at the fault plane. The thin lines in the 2D case from 0.1 to 0.5 distance units represent extrapolations of published results of Haskell (1969).